

profiles differ considerably from the out-of-vortex profiles, suggesting no or very little mixing until mid-April. That the vortex remains intact is also indicated by our diabatic trajectory calculation, and is in line with the meteorological analysis of Naujokat and co-workers (5) [*Polar Stratospheric Ozone, Proceedings of the Third European Workshop*, J. A. Pyle, N. R. P. Harris, G. T. Amanatidis, Eds. (European Communities, Luxembourg, 1996), p. 9] showing that the vortex remained stable until

late March followed by a slow transition to summertime conditions in April, but with a circulation reversal not accomplished before the end of the month.

37. S. J. Oltmans and D. J. Hofmann, *Nature* **374**, 146 (1995).
 38. We thank L. Froidevaux, H. Graf, P. Newman, W. Randel, S. Solomon, and three anonymous reviewers for very helpful discussions, R. van Dorland for a calculation of stratospheric cooling rates, and M.

Rex and P. von der Gathen for providing the Match results before publication. In part, this work was funded by the German Ministry of Education and Research (BMBF) under contract 01 LO 9221/4 (POLECAT) and 01 LO 9401 (MIPAS-B) and by the European Union under contract ENVCT95-0050 (TOPOZ), EV5VCT93-0331 (SESAME), and ENVCT95-0155 (STREAM).

30 November 1998; accepted 15 February 1999

Decay of the GRB 990123 Optical Afterglow: Implications for the Fireball Model

Alberto J. Castro-Tirado,^{1,5*} María Rosa Zapatero-Osorio,²
 Nicola Caon,² Luz Marina Cairós,² Jens Hjorth,³
 Holger Pedersen,³ Michael I. Andersen,⁴ Javier Gorosabel,⁵
 Corrado Bartolini,⁶ Adriano Guarnieri,⁶ Adalberto Piccioni,⁶
 Filippo Frontera,^{7,8} Nicola Masetti,⁸ Eliana Palazzi,⁸ Elena Pian,⁸
 Jochen Greiner,⁹ Renè Hudec,¹⁰ Ram Sagar,¹¹ Anil K. Pandey,¹¹
 Vinay Mohan,¹¹ Ramakant K. S. Yadav,¹¹ Nilakshi,¹¹
 Gunnlaugur Björnsson,¹² Páll Jakobsson,¹² Ingunn Burud,¹³
 Frederic Courbin,¹³ Gaetano Valentini,¹⁴ Anna Piersimoni,¹⁴
 Jesús Aceituno,¹⁵ Luz María Montoya,¹⁵ Santos Pedraz,¹⁵
 Roland Gredel,¹⁵ Charles F. Claver,¹⁶ Travis A. Rector,¹⁶
 James E. Rhoads,¹⁶ Fabian Walter,¹⁷ Jürgen Ott,¹⁸
 Hans Hippelein,¹⁹ Victor Sánchez-Béjar,² Carlos Gutiérrez,²
 Alejandro Oscoz,² Jin Zhu,²⁰ Jiansheng Chen,²⁰ Haotong Zhang,²⁰
 Jianyan Wei,²⁰ Aiyng Zhou,²⁰ Sergei Guziy,²¹
 Aleksei Shlyapnikov,²² John Heise,²³ Enrico Costa,²⁴
 Marco Feroci,²⁴ Luigi Piro²⁴

Broad-band (ultraviolet to near-infrared) observations of the intense gamma ray burst GRB 990123 started ~8.5 hours after the event and continued until 18 February 1999. When combined with other data, in particular from the Robotic Telescope and Transient Source Experiment (ROTSE) and the Hubble Space Telescope (HST), evidence emerges for a smoothly declining light curve, suggesting some color dependence that could be related to a cooling break passing the ultraviolet-optical band at about 1 day after the high-energy event. The steeper decline rate seen after 1.5 to 2 days may be evidence for a collimated jet pointing toward the observer.

Gamma-ray bursts (GRBs) are brief flashes of cosmic high energy (~10 keV–10 GeV) photons. They have remained without any satisfactory explanation since their discovery in 1967 (1). With the advent of the Italian-Dutch x-ray satellite BeppoSAX, it is possible to conduct deep counterpart searches only a few hours after a burst. This led to the first detection of x-ray and optical afterglows for GRB 970228 (2). Subsequent observations have shown that about half of the well-localized GRBs can be associated with optical emission, that gradually fades away, over weeks to months (3). About 10 such cases are known. Models proposed before the first detection of optical afterglow (4) have been successful in describing the decline of the optical emission. The afterglow is modeled as

due to synchrotron radiation from relativistically expanding matter, that collides with the interstellar medium.

GRB 990123 was detected at 09:47 universal time (UT) on 23 January 1999 by the GRB monitor (GRBM) and the wide-field camera (WFC) of BeppoSAX, and by three instruments on board the Compton Gamma-ray Observatory, the Burst and Transient Source Experiment (BATSE), the Compton Telescope (COMPTEL), and the Oriented Scintillation Spectrometer Experiment (OSSE). A complex light curve was obtained, lasting ~100 s (5). The γ -ray fluence was $\sim 5.1 \times 10^{-7} \text{ J m}^{-2}$ (6). This places the burst in the top 0.3 % of the BATSE GRB fluence distribution and it is one of the brightest events within the COMPTEL and OSSE range (>0.7 MeV) (7).

After 6.0 hours, BeppoSAX was reoriented toward the burst location and a previously unknown x-ray source was detected (8). The source intensity, $1.6 (\pm 0.2) \times 10^{-14} \text{ J m}^{-2} \text{ s}^{-1}$ (2 to 10 keV), makes this x-ray afterglow the brightest detected so far. Optical observation conducted in response to the location of the x-ray afterglow as determined by BeppoSAX led to the identification of an optical transient, the GRB optical afterglow (hereafter OA) (9), associated with the GRB. This OA was initially seen as an object of a red broad-band magnitude $R = 18.2$ (10). Optical observations had, however, begun much earlier. In response to the internet-transmitted trigger from BATSE, ROTSE at Los Alamos National Laboratories (11) had started wide-angle imaging 22 s after the beginning of the GRB. Off-line analysis, conducted after the above-mentioned identification, revealed that the OA had been detected already in the first exposure, and had peaked at visual broad-band magnitude $V \sim 9$, some seconds later.

Optical spectroscopic observations revealed that the redshift of the burst source is

¹Instituto de Astrofísica de Andalucía, IAA-CSIC, Granada, Spain. ²Instituto de Astrofísica de Canarias, La Laguna, Tenerife, Spain. ³Astronomical Observatory, University of Copenhagen, Copenhagen, Denmark. ⁴Nordic Optical Telescope, La Palma, Tenerife, Spain. ⁵Laboratorio de Astrofísica Espacial y Física Fundamental, INTA, Madrid, Spain. ⁶Dipartimento di Astronomia, Università di Bologna, Bologna, Italy. ⁷Dipartimento di Fisica, Università di Ferrara, Ferrara, Italy. ⁸Istituto Tecnologie e Studio Radiazioni Extraterrestri, CNR, Bologna, Italy. ⁹Astrophysikalisches Institut, Potsdam, Germany. ¹⁰Astronomical Institute, CZ-251 65 Ondrejov, Czech Republic. ¹¹U. P. State Observatory, Manora Park, Naini Tal, 263 129 India. ¹²Science Institute, University of Iceland, Reykjavik, Iceland. ¹³Institut d'Astrophysique et de Géophysique de Liège, Université de Liège, 4000 Liege, Belgium. ¹⁴Osservatorio Astronomico "V. Cerulli," Teramo, Italy. ¹⁵Calar Alto Observatory, Almería, Spain. ¹⁶Kitt Peak National Observatory, Tucson AZ, 85726, USA. ¹⁷Astronomical Observatory, University of Bonn, Germany. ¹⁸Radioastronomisches Institut, 53121 Bonn, Germany. ¹⁹Max-Planck Institut für Astronomie, Heidelberg, Germany. ²⁰Beijing Astronomical Observatory, Chinese Academy of Sciences, Beijing 100080, and Beijing Astrophysics Center, Beijing 100871, China. ²¹Nikolaev University Observatory, Nikolskaya, 24, 327030 Nikolaev, Ukraine. ²²Nikolaev Space Research Group, Nikolaev Astronomical Observatory, 327030 Nikolaev, Ukraine. ²³Space Research Organization Netherlands, Utrecht, The Netherlands. ²⁴Istituto di Astrofisica Spaziale, CNR, Frascati, Italy.

*To whom correspondence should be addressed E-mail: ajct@laeff.esa.es

REPORTS

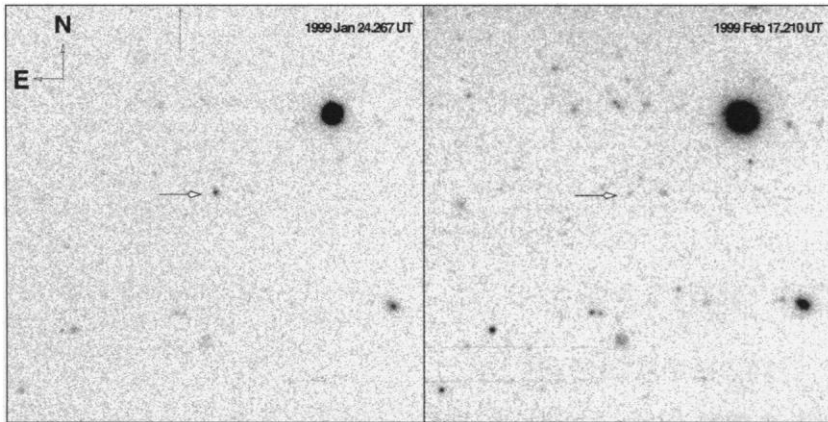


Fig. 1. Ultraviolet (*U* band) images of the OT 990123 location. The images were taken on 24 January, UT 04:35 (left panel, 18.8 hours after the GRB), and on 17 February, UT 05:00 (right panel, 24 days after the GRB). It shows the optical afterglow (arrow), and the underlying Galaxy at the center of the image. The field is 2.1 feet \times 2.1 feet. North is at top and east is to the left. Limiting magnitudes were $U \sim 22$, and $U \sim 24.5$, respectively.

$1.6 \leq z < 2.05$ (12, 13). Assuming isotropic emission, a Hubble constant of $H_0 = 70 \text{ km s}^{-1} \text{ Mpc}^{-1}$, and a cosmological density parameter $\Omega_0 = 0.3$, implies an energy release in γ -rays of $\sim 2.5 \times 10^{54}$ erg, using the BeppoSAX GBM data. This is larger by a factor of 10 to 100 than measured for any of the four other GRBs for which a redshift is known.

We have obtained optical and near-infrared (IR) images centered on the GRB location starting 8.5 hours after the burst (Table 1). For the optical images, photometry was performed by means of SExtractor (14), making use of the corrected isophotal magnitude, which is appropriate for star-like objects. As the OA was generally quite faint on the later epoch images, the DAOPHOT (15) profile-fitting technique was used for the magnitude determination. Zero points, atmospheric extinction and color terms were computed using

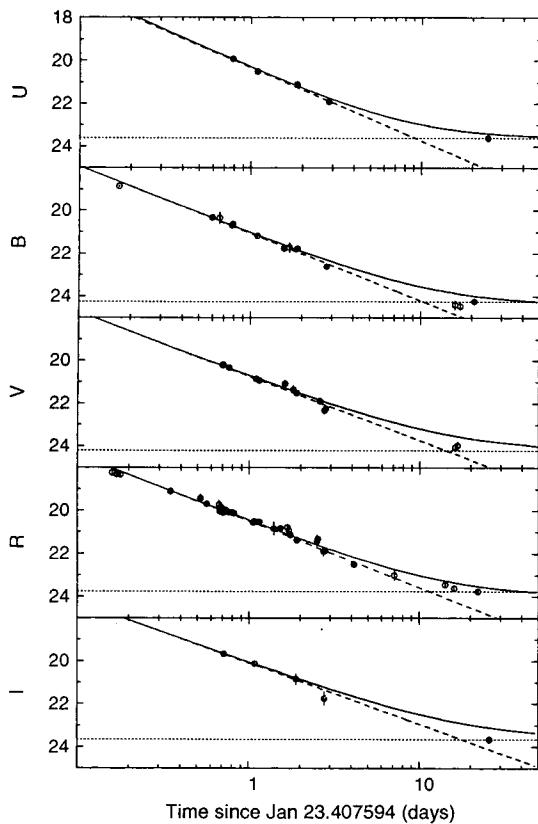


Fig. 2 (left). The *UBVRI*-band light-curves of the OA related to GRB 990123, including the underlying Galaxy. Filled circles are our data, and empty circles are data taken from the literature (23). The latter have been brought to a common reference system. The dashed line is the pure OA contribution to the total flux, according to the fits given on Table 4 for the period of 8 hours to 2 days. The solid line is the combined flux (OA plus underlying Galaxy).

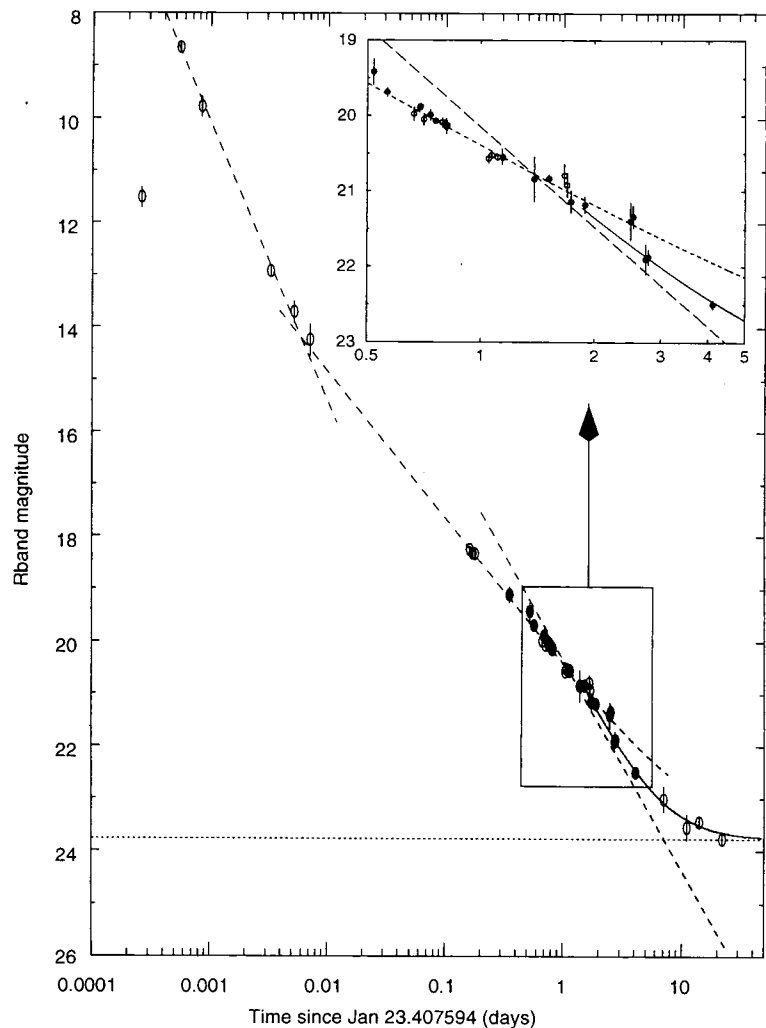


Fig. 3 (right). The *R*-band light-curve of the GRB 990123 OA. Based on our observations and other data reported elsewhere (11, 23). The diamond is the pure OA flux as derived from the HST observation (20). The dotted line is the contribution of the underlying Galaxy, with $R \sim 23.77 \pm 0.10$, from (21). The three dashed lines are the contribution of the OA, following $F \propto t^\delta$ with $\delta = -2.12$ up to ~ 10 min, $\delta = -1.13$ up to ~ 1.5 days, and $\delta = -1.75$ after that time (Table 3). The latter matches the OA flux as derived from the HST observation (20). The solid line, only drawn after 1.5 days for clarity is the total observed flux (OA + Galaxy).

REPORTS

observations of standard fields taken throughout the run. Magnitudes of the secondary standards in the GRB fields agree, within the uncertainties, with those given in (16). Zero point uncertainties are also included in the given errors. For the IR images, the *JK*-band calibration is based on the calibration given in (17).

A comparison among optical images acquired on 23 and 24 January allowed us to

confirm the variability in intensity of the proposed OA (10). When compared to stars in the field, the object shows an ultraviolet (UV) excess, further supporting the association of the transient x-ray source with the OA. About 8.5 hours after the burst, we measured $R = 19.10 \pm 0.15$ for the OA, and 19 hours later we found $R = 19.99 \pm 0.07$ and a broad-band UV magnitude of $U = 19.92 \pm 0.03$. In these images the object is point-like

(resolution ~ 1 inch) and there is no evidence of any underlying extended object as seen at later epochs (Fig. 1).

Our first optical observation was done nearly simultaneous to the BeppoSAX narrow-field instruments (NFI) observation, which began 6 hours after the burst, implying a ratio of x-ray (2 to 10 keV) to optical luminosity (*R*-band) ~ 10 , similar to GRB 970508 (18) but different from a ratio ~ 200 for GRB 970228 (19).

Our *UBVRI* light curve (Fig. 2) shows that the source was declining in brightness. To obtain the flux due to the OA we have excluded the contribution of the underlying galaxy that was detected with the Hubble Space Telescope (HST) (20). For the galaxy we have considered our broad-band measurements of $U = 23.60 \pm 0.15$ on 17.2 February, $B = 24.23 \pm 0.10$ (blue) on 13.2 February, and $I = 23.65 \pm 0.15$ (near-IR) on 18.2 February which, together with $V = 24.20 \pm 0.15$ on 9.1 February (20) and $R = 23.77 \pm 0.10$ on 14.5 February (21) imply a flat spectral distribution ($F_\nu \propto \nu^\beta$ with $\beta \sim 0$) as expected in the rest-frame UV for a star-forming galaxy (22).

A single power-law decay, as predicted by the single afterglow models, with the flux $F \propto t^{-\delta}$ where t is the time since the onset of the GRB (where the onset is arbitrarily defined on the basis of the BATSE data) and δ is the power-law decay exponent, does not fit the

Table 1. Journal of the GRB 990123 optical and IR observations.

Date (1999)	Time (UT)	Telescope	Filter	Integration time (s)	Magnitude
23 Jan	18:09	0.6 BAO	<i>R</i>	1200	19.10 ± 0.15
23 Jan	22:15	1.0 UPSO	<i>R</i>	1200	19.42 ± 0.17
23 Jan	23:00	1.0 UPSO	<i>R</i>	2400	19.69 ± 0.06
24 Jan	02:18	2.5 NOT	<i>R</i>	180	19.89 ± 0.04
24 Jan	02:23	2.5 NOT	<i>R</i>	180	19.88 ± 0.04
24 Jan	02:28	2.5 NOT	<i>V</i>	180	20.21 ± 0.06
24 Jan	02:33	2.5 NOT	<i>V</i>	180	20.18 ± 0.06
24 Jan	02:56	1.5 Loiano	<i>I</i>	1200	19.66 ± 0.14
24 Jan	03:24	1.5 Loiano	<i>R</i>	1500	19.99 ± 0.07
24 Jan	03:56	1.5 Loiano	<i>V</i>	1800	20.32 ± 0.07
24 Jan	03:59	2.5 NOT	<i>R</i>	6×300	20.07 ± 0.02
24 Jan	04:26	2.5 NOT	<i>B</i>	300	20.68 ± 0.03
24 Jan	04:35	2.5 NOT	<i>U</i>	600	19.92 ± 0.03
24 Jan	04:39	1.5 Loiano	<i>B</i>	2700	20.62 ± 0.08
24 Jan	05:11	1.5 Loiano	<i>R</i>	600	20.14 ± 0.10
24 Jan	06:20	0.8 IAC	<i>R</i>	900	≥ 19.5
24 Jan	06:36	0.8 IAC	<i>I</i>	900	≥ 19.0
24 Jan	11:56	4.0 KPNO	<i>U</i>	900	20.50 ± 0.10
24 Jan	19:07	0.6 BAO	<i>R</i>	3600	20.84 ± 0.30
24 Jan	22:14	1.0 UPSO	<i>R</i>	3600	20.83 ± 0.08
25 Jan	03:28	1.5 Loiano	<i>R</i>	2×1500	21.14 ± 0.15
25 Jan	04:30	2.2 CAHA	<i>R</i>	2×300	≥ 21.0
25 Jan	04:52	1.5 Loiano	<i>V</i>	2×1500	21.35 ± 0.18
25 Jan	06:25	2.5 NOT	<i>U</i>	2×600	21.11 ± 0.06
25 Jan	06:45	0.8 IAC	<i>R</i>	900	≥ 20.5
25 Jan	06:50	2.5 NOT	<i>B</i>	2×300	21.76×0.05
25 Jan	07:01	0.8 IAC	<i>I</i>	667	≥ 19.5
25 Jan	07:01	2.5 NOT	<i>V</i>	2×180	21.52 ± 0.07
25 Jan	07:10	2.5 NOT	<i>R</i>	2×180	21.18 ± 0.11
25 Jan	07:17	2.5 NOT	<i>I</i>	180	20.85 ± 0.25
25 Jan	21:30	0.6 BAO	<i>R</i>	2400	21.40 ± 0.25
25 Jan	22:33	1.0 UPSO	<i>R</i>	2400	21.34 ± 0.15
25 Jan	23:45	1.0 UPSO	<i>V</i>	3600	21.89 ± 0.20
26 Jan	03:19	1.5 Loiano	<i>R</i>	3×1500	21.90 ± 0.20
26 Jan	03:46	1.5 Loiano	<i>V</i>	2×1800	22.33 ± 0.17
26 Jan	03:55	3.5 CAHA	<i>I</i>	900	21.75 ± 0.30
26 Jan	04:23	3.5 CAHA	<i>R</i>	900	21.87 ± 0.10
26 Jan	04:41	3.5 CAHA	<i>B</i>	900	22.60 ± 0.10
26 Jan	05:03	3.5 CAHA	<i>V</i>	1200	22.24 ± 0.06
26 Jan	05:51	3.5 CAHA	<i>U</i>	2×1800	21.90 ± 0.15
27 Jan	12:34	4.0 KPNO	<i>R</i>	5×900	22.50 ± 0.05
28 Jan	02:35	2.2 CAHA	<i>U</i>	2×1500	≥ 21.0
28 Jan	03:18	2.2 CAHA	<i>I</i>	1500	≥ 22.0
29 Jan	23:15	1.0 UPSO	<i>R</i>	6×1200	≥ 22.5
13 Feb	05:00	2.5 NOT	<i>B</i>	18×600	24.23 ± 0.10
17 Feb	05:00	2.5 NOT	<i>U</i>	8×1200	23.60 ± 0.15
18 Feb	05:00	2.5 NOT	<i>I</i>	10×900	23.65 ± 0.15
24 Jan	05:30	1.5 TCS	<i>J</i>	1340	≥ 18.4
24 Jan	06:03	1.5 TCS	<i>K'</i>	450	≥ 17.5
30 Jan	05:50	3.5 CAHA	<i>K'</i>	2310	≥ 19.5

Observations were conducted at the 0.6-m Schmidt telescope of the Beijing Astronomical Observatory in Xinglong, China (BAO); the 1.04-m Sampurnanand telescope at Uttar Pradesh State Observatory, Nainital, India (UPSO); the IAC 0.82-m telescope at Observatorio del Teide, Tenerife, Spain (IAC); the 2.56-m Nordic Optical Telescope at Observatorio del Roque de los Muchachos, La Palma, Spain (NOT); the 1.5-m telescope of the Bologna Astronomical Observatory at Loiano, Italy (Loiano); the 3.5-m telescope at the German-Spanish Calar Alto Observatory (3.5CAHA); the 2.2-m telescope at the German-Spanish Calar Alto Observatory (2.2CAHA); the 4.0-m telescope at the Kitt Peak National Observatory (KPNO); and the 1.5-m Carlos Sánchez Telescope at the Observatorio del Teide, Tenerife, Spain (TCS).

Table 2. Power-law fits to the *UBVRI* observations of GRB 990123 for $t > 3$ hours.

Filter	δ	χ^2/df
<i>U</i>	-1.41 ± 0.07	3.0/2
<i>B</i>	-1.33 ± 0.05	11.8/7
<i>V</i>	-1.30 ± 0.03	22.5/10
<i>R</i>	-1.21 ± 0.02	99.2/33
<i>I</i>	-1.32 ± 0.19	1.9/2

Table 3. Power-law fits to the *R*-band observations of GRB 990123.

Time interval	δ	χ^2/df
0 – 10 min	-2.12 ± 0.03	15.9/3
3 hours – 2 days	-1.13 ± 0.02	23.2/25
2 – 20 days	-1.75 ± 0.11	2.1/7

Table 4. Power-law fits to the *UBVRI* observations of GRB 990123 for 8 hours to 2 days.

Filter	δ	χ^2/df
<i>U</i>	-1.36 ± 0.08	3.7/1
<i>B</i>	-1.26 ± 0.06	5.4/6
<i>V</i>	-1.20 ± 0.04	5.8/8
<i>R</i>	-1.13 ± 0.02	23.2/25
<i>I</i>	-1.14 ± 0.19	0.1/1

data obtained beginning 3 hours after the burst (as can be seen from the high χ^2 per degree of freedom (df) values in Table 2). We also included in the fit other observations given in the literature (23), normalized to a common reference system. The results are even worse if we consider the ROTSE data (11) and the magnitude derived from the HST observation on 9.1 February (20). This implies that a single power law is not the best model.

The ROTSE and HST points can be transformed to the *R*-band magnitudes by assuming that $V-R \sim 0.3$ (based on our earliest and latest observations). Then we find that the overall *R*-band light curve is better sampled than the other bands and can be fit when three distinct power-law decays are considered, especially from the time intervals of 3 hours to 2 days and of 2 days to 20 days after the burst (Fig. 3 and Table 3). Therefore, for the rest of the broad-band data and due to the lack of measurements after 2 days, we have performed fits only from the time interval of 8 hours to 2 days after the burst (Table 4). The *BVRI* band fits are more acceptable than those given in Table 2. Although suggestive of a temporal decay rate gradual change, the multicolor fit is consistent, within a 2 s uncertainty, with a single power law with $\langle\delta\rangle = -1.22 \pm 0.08$.

GRB optical afterglows can be explained by the “standard” fireball model (24), under the assumption of an impulsive energy input characterized by a given energy and a bulk Lorentz factor. A forward relativistic blast wave is moving ahead of a fireball and sweeps up the interstellar matter, decelerating with time, and producing an afterglow at frequencies gradually declining from x-rays to visible and radio wavelengths. The properties of the blast wave can be derived from the classical synchrotron spectrum (25) produced by a population of electrons with the addition of self absorption at low frequencies

and a cooling break (26). The population of electrons has a power-law distribution of Lorentz factors Γ_e following $dN/d\Gamma_e \propto \Gamma_e^{-p}$ (above a minimum Lorentz factor $\Gamma_e \geq \Gamma_m$, corresponding to the synchrotron frequency ν_m), where p is the usual index of the electron energy distribution.

According to the current view, the forward external shock wave would have led to the afterglow as observed in all wavelengths (27). On 24.2 January UT, the equivalent spectral slope β (with $F_\nu \propto \nu^\beta$) between the optical band and the x-ray wavelengths was $\beta_{\text{opt}} = -0.68 \pm 0.05$ (Fig. 4), in agreement with the optical spectroscopy obtained on the same date (13) and similar to the spectral indexes of other x-ray afterglows in which $\beta_{\text{opt}} \approx -0.5$ to -1.0 (28). Our nearly-simultaneous *UBVRI* observations and the upper limits (Table 1) for the *J* and *K* band measurements on 24.2 January UT, imply $R-J \leq 1.6$, $R-K \leq 2.8$, and are in agreement with the above-mentioned values of β_{opt} , indicating a non-reddened spectrum.

The optical afterglow is fit by a single power law up to $t \approx 1.5$ –2 days. Thereafter, a different, steeper power-law index fits the data better than a single power law. A possible explanation for the possible gradual change of δ between ~ 8 hours and 2 days in the *UBVRI* bands could be the passage of the cooling frequency across the UV-optical range at ~ 1 day. Assuming an adiabatic blast wave and that the cooling frequency ν_c was above the UV on 24.2 January, we can consider $F_\nu \propto \nu^{-0.7}$ (for $\nu < \nu_c$) as observed in our spectrum taken on 24.2 January (12). This implies a temporal decay $F_\nu \propto t^{-1.05}$ for $\nu < \nu_c$ and $F_\nu \propto t^{-1.3}$ for $\nu > \nu_c$, with a slow transition from one behavior to the other ($\nu_c \propto t^{-0.5}$). This transition could have been hinted in our measurements (Table 4). With respect to the break seen after 1.5 to 2 days, a possibility will be the transition for spherical ejecta to a non-relativistic phase (13). An alternative explanation might be the existence

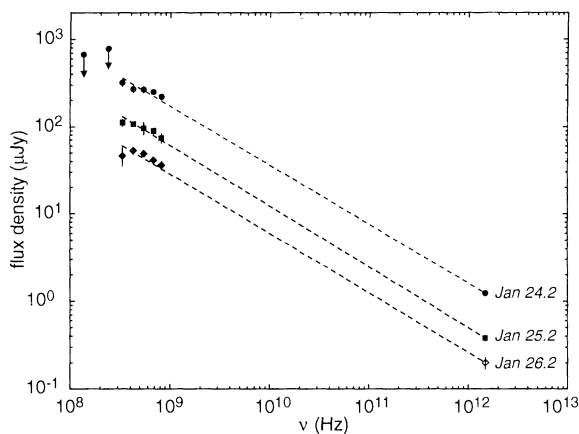
of a strongly collimated jet pointing toward us that has begun to spread (29), although this cannot be definitively proven on the basis of the polarimetric measurements (30).

The observed power law with $\delta = -1.75 \pm 0.11$ is also expected from seeing the edge of the jet (31), which occurs well before the jet expands laterally from the point of view of Earth-based observers (32). The break due to a lateral expansion in the decelerating jet occurs when the initial Lorentz factor Γ drops below θ_0^{-1} (with θ_0 the initial opening angle). For the latter a change in δ from $3(1-p)/4$ to $-p$ (for $\nu_m < \nu < \nu_c$), or from $(2-3p)/4$ to $-p$ (for $\nu \geq \nu_c$) is expected. From the x-ray (2 to 10 keV) data obtained after 6 hours, $\delta_x = -1.44 \pm 0.07$ was derived (33), which implies $p = 2.58 \pm 0.10$ for the fast cooling electrons. And from $\delta_R = -1.13 \pm 0.02$ in the *R*-band, we should get $p = 2.50 \pm 0.03$ (2.17 ± 0.03) for the slow (fast) cooling electrons. Then we consider $p = 2.50 \pm 0.03$ and consequently, the OT light curve may continue to steepen, ultimately approaching a slope $\delta \sim -2.5$.

References and Notes

1. For an extensive review of GRB observations, see G. J. Fishman and C. A. Meegan, *Annu. Rev. Astron. Astrophys.* **33**, 415 (1995).
2. E. Costa et al., *Nature* **387**, 783 (1997); J. van Paradijs et al., *Nature* **386**, 686 (1997).
3. A. J. Castro-Tirado, *Astrophysics and Space Science*, in press, preprint available at <http://xxx.lanl.gov/abs/astro-ph/9903187>.
4. P. Mészáros and M. J. Rees, *Astrophys. J.* **476**, 232 (1997); R. A. M. J. Wijers, M. J. Rees, P. Mészáros, *Mon. Not. R. Astron. Soc.* **288**, L51 (1997); E. Waxman, *Astrophys. J.* **491**, L19 (1997); D. E. Reichart, *Astrophys. J.* **485**, L57 (1997).
5. L. Piro et al., *GCN Circular* 199 (1999); M. Feroci et al., *IAU Circular* 7095 (1999).
6. R. M. Kippen et al., *GCN Circular* 224 (1999).
7. A. Connors, R. M. Kippen, C. A. Young, S. Barthelmy, P. Butterworth, *GCN Circular* 230 (1999); S. Matz, G. H. Share, R. Murphy, J. D. Kurfess, *GCN Circular* 231 (1999).
8. L. Piro et al., *GCN Circular* 203 (1999); J. Heise et al., *IAU Circular* 7099 (1999).
9. For OA we refer to a rapidly varying (usually declining) point source seen at optical wavelengths and never detected in the past. See also R. Hudec, *Astrophys. Lett. Comm.* **28**, 359 (1993).
10. S. C. Odewahn et al., *IAU Circular* 7094 (1999).
11. C. W. Akerlof and T. A. McKay, *IAU Circular* 7100 (1999); C. W. Akerlof et al., *Nature*, in press.
12. M. I. Andersen et al., *Science* **283**, 2075 (1999).
13. S. R. Kulkarni et al., *Nature*, in press.
14. E. Bertin and S. Arnouts, *Astron. Astrophys.* **117**, 393 (1996).
15. P. B. Stetson, *Publ. Astron. Soc. Pacific* **99**, 191 (1987).
16. Nilakshi, R. K. S. Yadav, V. Mohan, A. K. Pandey, R. Sagar, *GCN Circular* 252 (1999); Nilakshi, R. K. S. Yadav, V. Mohan, A. K. Pandey, R. Sagar, *Bull. Astron. Soc. India*, in press.
17. H. Guetter, F. Vrba, A. Henden, private communication (1999). They observed a nearby star under photometric conditions just before observing the GRB 990123 field.
18. A. J. Castro-Tirado et al., *Science* **279**, 1012 (1998).
19. A. Guarnieri et al., *Astron. Astrophys.* **328**, L13 (1997).
20. A. Fruchter et al., *GCN Circular* 255 (1999); A. Fruchter et al., in preparation, preprint available at <http://xxx.lanl.gov/abs/astro-ph/9902236>.
21. J. Halpern, Y. Yadigaroglu, K. M. Leighly, J. Kemp, *GCN Circular* 257 (1999).

Fig. 4. The multiwavelength spectrum of GRB 990123 on 24 to 26 January 1999 UT. The two first x-ray data points (24.2 January and 25.2 January) are the BeppoSAX NFI measurements obtained at that time. The third one is the extrapolation following the power-law decay seen in x-rays, from (33). Circles are the data obtained on 24.2 January UT, squares are the data obtained on 25.2 January UT, and diamonds are the data obtained on 26.2 January UT. The correction for galactic extinction has been considered taking into account $E(B - V) = 0.016$ from (34). A fit to the optical to x-ray spectral flux density is consistent on the three dates with $\beta = -0.68 \pm 0.05$.



Polarimetric Constraints on the Optical Afterglow Emission from GRB 990123

Jens Hjorth,^{1*} Gunnlaugur Björnsson,² Michael I. Andersen,³
 Nicola Caon,⁴ Luz Marina Cairós,⁴
 Alberto J. Castro-Tirado,^{5,6} María Rosa Zapatero Osorio,⁴
 Holger Pedersen,¹ Enrico Costa⁷

Polarization of the optical emission from GRB 990123 was measured on 24.17 January 1999 universal time with the Nordic Optical Telescope. An upper limit of 2.3% on the linear polarization was found. Accurate polarization measurements provide important clues to the blast wave geometry and magnetic field structure of gamma-ray bursts (GRBs). The lack of detectable polarization for GRB 990123 indicates that the optical afterglow was produced by a blast wave of unknown geometry with an insignificant coherent magnetic field or by a beamed outflow at high Lorentz factor seen at a small viewing angle. Such a collimated jet would help solve the problem of energy release in this exceptionally luminous cosmological burst.

Optical afterglow, observed following nine γ -ray bursts over the past 2 years, is believed to be synchrotron radiation from an expanding ultrarelativistic blast wave (1). The exact source geometry and emission mechanism is unknown but can be constrained by accurate optical polarization measurements. Polarization may be expected if the emission is beamed or originates in a magnetic field produced by the blast wave with a coherence length growing at the speed of light.

GRB 990123 was a very bright GRB (2) accompanied by a $V \approx 9$ optical flash (3). The afterglow was the brightest ever recorded in x-rays (2) and sufficiently bright at optical wavelengths (4) to allow detailed ground-based observations (5, 6). This led to constraints on its redshift $1.60 \leq z < 2.05$ (6, 7), making it the intrinsically most luminous GRB observed to date with an inferred isotropic energy release in γ rays alone of about $E_\gamma \pi/\Omega \sim 4 \times 10^{54}$ erg (6), comparable only to GRB 980329, if that burst occurred at $z \sim 5$ (8).

As soon as the location of the optical afterglow of GRB 990123 became visible at the 2.56-m Nordic Optical Telescope (NOT) on La

Palma, The Canary Islands, observations designed to detect any polarization at the 10% level with high confidence were conducted. Polarimetric imaging observations were obtained with the Andalucia faint object spectrograph (ALFOSC) using two calcite blocks together with a red (R) broad-band filter (wavelength range: 5670 Å to 7150 Å). Each exposure gave two orientations of the polarization, 0° and 90°, or -45° and 45° (Table 1 and Fig. 1).

The linear polarization was computed from the derived fluxes in the four orientations. Assuming that no instrumental polarization or other systematic bias was present, the resulting linear polarization is $0.6 \pm 1.4\%$. If the polarization is determined relative to the two stars present in the field of view (Fig. 1) a maximum of $1.2 \pm 1.4\%$ linear polarization is found. Under the assumption that the two stars are unpolarized, the latter measurement would account for possible interstellar polarization, polarization induced by the telescope and instrument, and point-spread function (PSF) variation across the field. At such low significance levels a correction must be applied to the computed values to account for the non-Gaussian nature of the underlying probability distribution (9). When corrected for this effect the polarization is found to be $0.0 \pm 1.4\%$ using either measurement. This is consistent with no linear polarization and we conclude that an upper limit of 2.3% (95% confidence limit) is set on the linear polarization of the optical afterglow of GRB 990123 on 24.17 January 1999 universal time (UT). This upper limit is much stronger than the existing upper limits on the linear polarization of radio afterglows of cosmological GRBs; $<19\%$ for GRB 980329 (10) and $<8\%$ for GRB 980703 (11).

The effects of depolarization or interstellar polarization in the Galaxy are expected to be

22. J. S. Bloom *et al.*, in preparation, preprint available at <http://xxx.lanl.gov/abs/astro-ph/9902182>.
23. T. Galama *et al.*, *Nature*, in press; R. Gal *et al.*, *GCN Circular 207* (1999); V. Sokolov *et al.*, *GCN Circular 209* (1999); E. Ofek and E. Leibowitz, *IAU Circular 7096* (1999); E. Falco, C. Petry, C. Impey, A. Koekemoer, J. Rhoads, *GCN Circular 214* (1999); P. Garnavich, S. Jha, K. Stanek, M. Garcia, *GCN Circular 215* (1999); W. Offut, *IAU Circular 7098* (1999); L. A. Antonelli, A. Di Paola, G. Gandolfi, *GCN Circular 229* (1999); L. A. Antonelli, A. Di Paola, R. Speziali, G. Gandolfi, *GCN Circular 232* (1999); J. S. Bloom *et al.*, *GCN Circular 240* (1999); I. A. Yadigaroglu and J. Halpern, *GCN Circular 242* (1999); I. A. Yadigaroglu and J. Halpern, *GCN Circular 248* (1999); C. Veillet, *GCN Circular 253* (1999); C. Veillet, *GCN Circular 255* (1999); J. S. Bloom *et al.*, *GCN Circular 206* (1999).
24. For a review see T. Piran, *Physics Reports*, in press, preprint available at <http://xxx.lanl.gov/abs/astro-ph/9810256>.
25. V. L. Ginzburg and S. I. Syrovatskii, *Ann. Rev. Astron. Astrophys.* **3**, 297 (1965).
26. If the electrons are energetic they will cool rapidly for a cooling frequency $\nu_c < \nu_m$, and low energy electrons will have always slow cooling for $\nu_c > \nu_m$. See R. Sari, T. Piran, and R. Narayan, *Astrophys. J.* **497**, L17 (1998).
27. R. Sari and T. Piran, in preparation, preprint available at <http://xxx.lanl.gov/abs/astro-ph/9902009>.
28. T. Galama *et al.*, *Astrophys. J.* **500**, L97 (1998); J. Halpern *et al.*, *Nature* **393**, 41 (1998); A. J. Castro-Tirado *et al.*, *Astrophys. J.* **502**, L111 (1999).
29. J. Rhoads, *Astrophys. J.* **487**, L1 (1997).
30. J. Hjorth *et al.*, *Science* **283**, 2073 (1999).
31. P. Mészáros and M. J. Rees, *Mon. Not. R. Astron. Soc.*, in press, preprint available at <http://xxx.lanl.gov/abs/astro-ph/9902367>.
32. A. Panaitescu and P. Mészáros, in preparation, preprint available at <http://xxx.lanl.gov/abs/astro-ph/9806016> (1998).
33. J. Heise *et al.*, *Nature*, in press.
34. D. J. Schlegel, D. P. Fikbeiner, M. Davis, *Astrophys. J.* **500**, 525 (1998).
35. We thank A. Henden, F. Vrba, and H. Guetter for having provided the *J*- and *K*-band magnitudes for three local standards in the field; A. Alberdi, M. Ma's-Hesse, A. Rao, M. de Santos, P. Ruiz-Lapuente, M. Valdez-Gutiérrez, R. A. M. J. Wijers and A. Yoshida for very fruitful conversations; and the anonymous referees for useful suggestions. The Calar Alto German-Spanish Observatory is operated jointly by the Max-Planck Institut für Astronomie in Heidelberg, and the Comisión Nacional de Astronomía, Madrid. The Loiano Telescope is operated by Osservatorio Astronomico di Bologna and Università di Bologna. The Nordic Optical Telescope is operated on the island of La Palma jointly by Denmark, Finland, Iceland, Norway, and Sweden, in the Spanish Observatorio del Roque de los Muchachos of the Instituto de Astrofísica de Canarias. Kitt Peak National Observatory, National Optical Astronomy Observatories, is operated by the Association of Universities for Research in Astronomy, Inc. (AURA) under cooperative agreement with the National Science Foundation. We also acknowledge the Time Allocation Committees of Calar Alto, Roque, and Teide observatories. The operation of BAO 0.6-m Schmidt telescope is supported by the Chinese Academy of Sciences. The Beijing Astrophysics Center is jointly sponsored by the Chinese Academy of Sciences and Peking University. J.G. is supported by the Deutsche Agentur für Raumfahrtangelegenheiten (DARA). C.B., A.G., and A.P. acknowledge the support by the Università di Bologna (funds for selected research topics). The work of J.Z. is partly supported by the Pandeng Foundation of China, the Chinese National Natural Science Foundation. I.B. and F.C. are supported by contracts ARC94/99-178 "Action de Recherche Concertée de la Communauté Française" (Belgium) and "Pôle d'Attraction Interuniversitaire" P4/05 (SSTC, Belgium). This research was supported by the Danish Natural Science Research Council (SNF), the Icelandic Council of Science, and the University of Iceland Research Fund. The BeppoSAX team acknowledges support from the Italian Space Agency.

19 February 1999; accepted 8 March 1999

¹Astronomical Observatory, University of Copenhagen, Juliane Maries Vej 30, DK-2100 Copenhagen Ø, Denmark. ²Science Institute, University of Iceland, Dunhaga 3, IS-107 Reykjavik, Iceland. ³Nordic Optical Telescope, Ap. 474 St. Cruz de La Palma, E-38700 Canarias, Spain. ⁴Instituto de Astrofísica de Canarias, E-38200 La Laguna, Tenerife, Spain. ⁵Laboratorio de Astrofísica Espacial y Física Fundamental, Instituto Nacional de Técnica Aeroespacial, P.O. Box 50727, E-28080 Madrid, Spain. ⁶Instituto de Astrofísica de Andalucía, Consejo Superior de Investigaciones Científicas, P.O. Box 03004, E-18080 Granada, Spain. ⁷Istituto di Astrofisica Spaziale-C.N.R., Via Fosso del Cavaliere, I-00133 Rome, Italy.

*To whom correspondence should be addressed. E-mail: jens@astro.ku.dk